Correlation of DWI and DCE MRI Markers for the Study of Perfusion of the Lower Limb in Patients with Peripheral Arterial Disease

Georgios S. Ioannidis
Computational BioMedicine Laboratory (CBML), Institute of Computer Science (ICS) Foundation for Research and Technology – Hellas
Heraklion, Greece
grs.ioannidis@gmail.com

Katerina Nikiforaki
Computational BioMedicine Laboratory (CBML), Institute of Computer Science (ICS) Foundation for Research and Technology – Hellas
Heraklion, Greece
kat@ics.forth.gr

Apostolos Karantanas
Department of Medical Imaging
University Hospital
Heraklion, Greece
Department of Radiology Medical School University of Crete
Heraklion, Greece
karantanas@uoc.gr

***Abstract*— The aim of the present work is to correlate perfusion information obtained from semi-quantitative DCE data analysis with quantitative diffusion data analysis in patients with peripheral arterial disease. An in-house built software deploying linear and nonlinear least squares algorithms, was used for the quantification of the parameters based on intra-voxel incoherent motion (IVIM) model and exponentially modified Gaussian function. All numerical calculations were implemented in Python 3.5. Derived perfusion parameters (micro-perfusion fraction f and Wash-In respectively) showed good correlation (>0.5). This constitutes a promising result for obtaining perfusion information from DWI sequences without the need for contrast agent in patients with vascular disease.**

Keywords— diffusion weighted imaging, dynamic contrast enhanced imaging, peripheral arterial disease, intra–voxel incoherent motion, tissue perfusion, Pearson correlation

I. INTRODUCTION

Dynamic contrast enhanced magnetic resonance imaging (DCE-MRI) is a well-established method for the study of tissue perfusion, vascular permeability and expansions of extravascular-extracellular spaces (EES) [1],[2] in a minimally invasive way. It comprises a series of dynamic acquisitions during the first pass of paramagnetic contrast agent (CA) in order to produce signal intensity time curves. Proper mathematical models have been proposed for the extraction of clinically relevant perfusion parameters.

Diffusion Weighted Imaging (DWI) is one of the most commonly used techniques for the study of tissue properties both in terms of cellularity but also vascularity. Similarly to DCE, DWI is a 4D acquisition, composed of multiple 3D volumes acquired with different degree of diffusion sensitivity (by adjusting b-value (s/mm^2)). Proposed mathematical models such as the IVIM model described in [3], [4] can decompose perfusion information from diffusion signal contribution and result in markers indicative of tissue perfusion from properly designed DWI protocols. DWI contrast mechanism is the random walk (Brownian motion) of the water molecules in tissue and thus does not require the injection of CA, as opposed to DCE. Specifically, parameter f in (1) is indicative of microcirculation fraction in tissue volume and is used for the study of DWI based perfusion.

Since both imaging methods convey information on tissue perfusion and vascularity, several published works have studied the correlation of DCE and DWI markers mainly in the field of oncology [5]–[9]. Accordingly, patients with atherosclerotic vascular disease such as peripheral arterial disease [10] (PAD) undergo imaging examination for the assessment of lower limb perfusion as they run high risk for disease related complications (ischemic rest pain, gangrene or ischemic ulcers), leading to critical limb ischemia (CLI) [11]. Moreover, MRI can be the imaging modality of choice as it can monitor vascular disease with zero ionizing radiation dose and can be repeated frequently in order to detect possible vascular occlusion requiring prompt therapeutic intervention.

Certain restrictions apply to the use of CA in order to prevent any risks that could potentially be associated with gadolinium brain deposition [12] according to the European Medicines Agency (EMA). In this direction the avoidance of CA injection without any compromise in the diagnostic information would be beneficial for all patients undergoing MRI examinations.

The present study addresses the clinical question of the possible correlation between perfusion parameters derived from quantitative DWI and semi-quantitative DCE analyses and whether the former can provide clinically useful tissue perfusion information. Quantitative modeling refers to parameters calculated directly from physiology based models such as (6) and (7) while, the term semi-quantitative is used for data driven markers. Previous works have verified the correlation between semi-quantitative DCE methods with IVIM, more specifically the relative enhancement ratio (RER) with f-IVIM [13]. In this context our intention is to examine the correlation of f-IVIM with other DCE derived markers, i.e. Wash-In (WIN). Both semi-quantitative DCE markers, WIN and RER, refer to the rate of change of the

This research is co-financed by Greece and the European Union (European Social Fund-ESF) through the Operational Programme «Human Resources Development, Education and Lifelong Learning 2014-2020» in the context of the project "Newer techniques in MR Imaging of musculoskeletal disorders" (MIS 5004349).

CA's inflow. However, WIN is less prone to miscalculation errors as its calculation is based on analytical expressions rather than raw signal intensity in two successive time points used in RER calculation (section II.D).

Possible correlation between WIN and f will enhance the diagnostic evidence concerning the use of DWI for the study of tissue perfusion in cases where CA administration is contraindicated for clinical or other reasons (hardware, acquisition time or post processing constraints).

II. Materials and Methods

A. Patient Cohort

20 patients (11 males, 9 females) with PAD underwent MR examination of lower limb during a 2-year study period (2016-2018) at the local university hospital. The median age was 66 years (range 56-81 years). All patients presented with CLI and according to Fontaine classification [14], 7 patients had stage III and 13 patients stage IV PAD. Exclusion criteria were all common contraindications to MRI, including pacemakers, ferromagnetic implants and claustrophobia and also contraindications for administration of Gadolinium contrast medium such as renal insufficiency and allergy to gadolinium. The acquisition protocol was submitted and approved by the local ethics committee and all patients signed informed consent prior to examination, where the use of MRI data for scientific purposes was explicitly declared.

B. Imaging Protocol

Each of 20 patients underwent MR examination on a 1.5T clinical MR Scanner (Vision/Sonata Hybrid system, Siemens, Erlangen, Germany) upgraded with gradients (Strength: 45 mT/m, slew rate: 200 mT/m/ms), equivalent with those gradients operating on 3T systems.

As part of an advanced imaging protocol, DWI and DCE MRI quantitative techniques where suitably modified and added to the conventional sequences. Parasagittal imaging plane was chosen for the optimal depiction of arteries and veins of the lower limb. Diffusion data were acquired utilizing a high resolution HASTE (Half-Fourier Acquisition Single-shot Turbo spin Echo) sequence with diffusion sensitizing gradients with b-values [b = 0, 50, 100, 150, 200, 500, 800, 1000 s/mm^2], number of slices = 13, echo time (TE) =105 ms, repetition time (TR) = 2000 ms, matrix size =384×384, field of view (FOV)=250×250, slice thickness=5mm. DWI acquisition was repeated with, different polarization direction of the frequency encoding gradient (P-A instead of A-P in the initial acquisition (Anterior-Posterior)) [15]. The two data sets were averaged and the resulting image was used for the quantification process. The reason for the double acquisition is the reduction of machine related geometrical distortions or apparent distortions in signal intensities.

T1W DCE perfusion MR imaging of the lower limb was performed by utilizing a 3D VIBE (volume interpolated breath hold examination). An intravenous continual injection of the paramagnetic CA (Magnevist, Gadopentetate Dimeglumine, Bayer Healthcare, Bayer, 0.1 mmol/kg) was administered for approximately one minute. The aforementioned T1W DCE VIBE perfusion sequence was continuously repeated for ten minutes (20 secs temporal resolution) after the intravenous injection of the CA with the following imaging parameters: FA = 15°, TE =2.73 ms, TR=7.8 ms, matrix size=512×512 and FOV=250×250. The total volume coverage was 26 space filling slices of 3 mm slice thickness. The selected volume coverage was considered adequate for the depiction of lower limb arteries and veins that might be related to blood supply to the ischemic regions of interest.

C. DWI Analysis

DWI and DCE related parameters were quantified by an in-house platform written in python 3.5. The trust region reflective algorithm "least_squares" [16] was used for the extraction of the parametric maps suitable for solving nonlinear bound-constrained minimization problems as defined in the SciPy.optimize library [17].

IVIM model, is an extension of the mono-exponential diffusion model expressed in (1) [18] and relates to the microscopic displacement of the water molecules due to diffusion and capillary perfusion. The DWI signal decay as a function of b-value is expressed in (2).

$$S(b)/S(0) = e^{-bD} \quad (1)$$

$$S(b)/S(0) = (1-f)e^{-bD} + fe^{-bD^*} \quad (2)$$

S(b) represents the signal intensity at the current b-value and S(0) is the signal intensity without diffusion weighting (meaning b=0), D (mm^2/s) is the diffusion coefficient, D* (mm^2/s) is the pseudo-diffusion coefficient and f is fractional perfusion related to the microcirculation.

Fitting the IVIM model to the DWI data is mainly succeeded by two different fitting methods.

a) IVIM fitting method 1: The first method constitutes a direct estimation of the IVIM parameters (f,D,D*) using "least_squares" fitting algorithm with the following bounds for each parameter: $f \in (0,1), D \in (0,5) \times 10^{-3}\, mm^2/s$, $D^* \in (10,200) \times 10^{-3}\, mm^2/s$

b) IVIM fitting method 2: The second method is a dual step process combining linear and non-linear fitting algorithms. It has been previously shown that perfusion in the

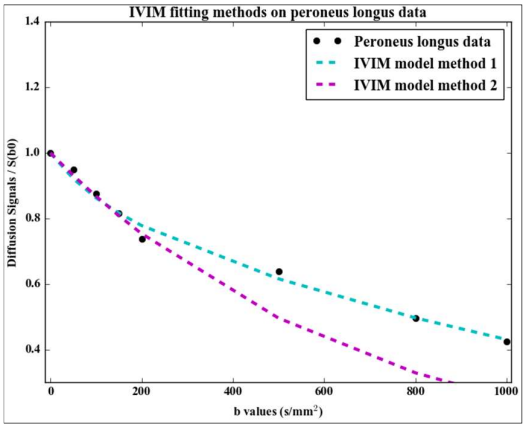

Fig. 1. IVIM fitting methods. Diffusion MR Signal of peroneus longus muscle data (dots) and fitted curves for IVIM model calculated by method 1 (cyan dashed line) and method 2 (magenda dashed line).

cappilary network is in presence at the low b-value range (typically for b-values < 200 s/mm^2) [19]. Thus, in the high b-value range (b>200 s/mm^2) the signal decay is considered to be monoexponential and as a first step, D is calculated by linear fitting "scipy.optimize.lsq_linear" to (1) after taking the logarithm of both sides. Since the diffusion coefficient D is determined, parameters f and D* are extracted from (2) by using the nonlinear fitting algorithm for all b-values. A fitting example of the two IVIM methods on peroneus longus muscle data is illustrated in Fig. 1.

D. DCE MRI semi-quantitative Analysis

For the calculation of WIN parameter, the signal intensity curves over time for every voxel in the temporal domain were fitted to the exponentially modified Gaussian (EMG) function (3) with four unknown parameters (a,b,c,d).

$$f(t) = \frac{ac\sqrt{2\pi}}{2d}\exp\left(\frac{b-t}{d} + \frac{c^2}{2d^2}\right)\left[\frac{d}{|d|} - \mathrm{erf}\left(\frac{b-t}{\sqrt{2c}} + \frac{c}{\sqrt{2d}}\right)\right] \quad (3)$$

More precisely, erf(t) is the Gaussian error function, $erf(t) = \int_{-t}^{t} e^{-x^2}\,dx$. The four unknown parameters a,b,c,d have not any physiological meaning and thus the optimization was performed in the range of real numbers ($\mathbb{R}$) with the Levenberg-Marquardt algorithm [20]. After fitting the EMG function to the PAD data a variety of semi-quantitative parameters can be computed with the use of the first derivative of the EMG function [21], [22] such as: WIN, WOUT, TTPK and TMSP. WIN and WOUT parameters were calculated as the maximum and minimum value of the EMG's function respectively. Their role is to describe the rate of change of the contrast agent's inflow and outflow. TTPK is the time required for the EMGs function to reach its maximum value while, TMSP (time to maximal slope) is the required time of the first derivative of (3) to reach its maximum value. A graphical illustration of the semi-quantitative parameters extraction is presented in Fig. 2.

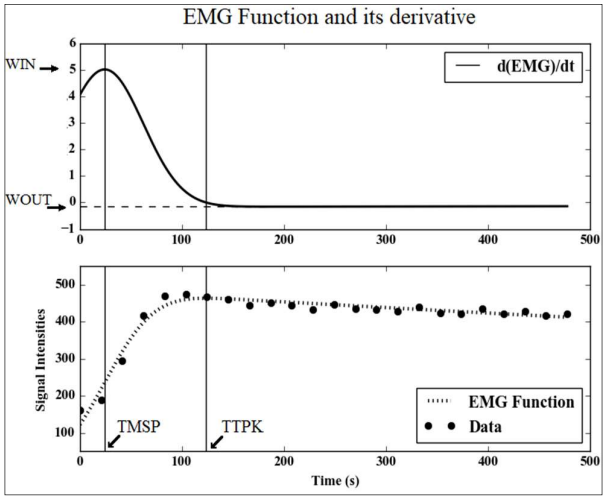

Fig. 2. Graphical illustration of semi-quantitative parameters from raw DCE data. [Lower image] Signal intensity data (dots) and EMG function fit (dashed line). Vertical lines depict the TMSP (time o maximal slope) and TTPK (time to peak) as defined above. [Upper image] The first derivative of the fitted EMG function and the extraction of WIN and WOUT

In general, the fitting process is affected by instrumentation noise resulting to parametric maps with large local variations within neighboring voxels. To this end, we applied a 5×5 Gaussian filter with $\sigma = 0.9$ on the derived parametric maps to reduce the effect of noise, as described in bibliography [8], [13].

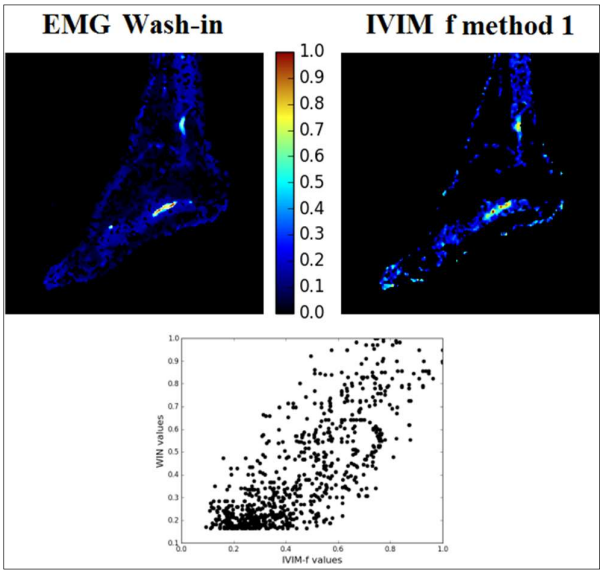

Fig. 3. DCE and DWI perfusion analysis of a patient with PAD. Parasagittal parametric map of the lower extremity showing Wash-In (WIN) calculated by EMG [upper left] and f-IVIM method 1 [upper right]. Both maps have been normalized to [0,1]. [Lower image:] q-q plot of WIN versus f-IVIM values.

E. Fitting Performance

The evaluation of the fitting performance for the semi-quantitative DCE and DWI analysis was based on the adjusted R squared ($\bar{R}^2$). This choice was considered advantageous over R^2 as it takes into account the R^2 and therefore the residual sum of squares between model and data points, the number of the explanatory variables (p) and the number of data time points (N). In more detail, $\bar{R}^2$ it is a given by the formula below:

$$\bar{R}^2 = 1 - (1 - R^2)\,\frac{N-1}{N-p-1} \quad (4)$$

F. Correlation Analysis

In order to use Pearson's correlation coefficient in 3D space an essential step is to resize DCE parametric maps to the matrix size of DWI images using bicubic interpolation. Additionally, DWI and DCE 4D data alignment is performed based on the image specific dicom tag of slice location in the z-axis (slice-axis). In order to focus on the study of perfusion of the lower limb we intended to exclude data from physiologically non perfused areas, such as bones, where WIN and IVIM-f are expected to be equal to zero. In the opposite case the large number of those values would contaminate the results by presenting false positive correlation corresponding to the zero values. Thus for every patient Pearson's correlation coefficient (r) was calculated by (5).

$$r_{f,WIN}\frac{\sqrt{\sum_{k=1}^{N}(f_k-\bar{f})\,(WIN_k-\overline{WIN})}}{\sqrt{\sum_{k=1}^{N}(f_k-\bar{f})^2}\sqrt{\sum_{k=1}^{N}(WI\ _k-\overline{WIN})^2}} \quad (5)$$

$\overline{WIN}$ and $\bar{f}$ represent the mean values of WIN and f respectively for each patient.

G. DCE MRI Quantitative Analysis

In order to understand the difference between quantitative and semi-quantitative perfusion models, in this paragraph the most widely used quantitative DCE models such as the extended Tofts (ETM) [23] and Patlak's (PM) [24] models are described. Considering the concentration of CA in the tissue $(C_t(t))$ and the concentration of CA in a feeding artery $(C_a(t))$, also known as the arterial input function (AIF), ETM assumes bidirectional transfer of the CA between the blood plasma and the extravascular-extracellular space (EES) as seen in (6) below:

$$C_t(t) = K^{trans}e^{-K_{ep}t} \circledast C_a(t) + v_p C_a(t) \quad (6)$$

where, K^{trans} (min^{-1}) represents the transfer constant from the blood plasma into the EES and K_{ep} (min^{-1}) represents the transfer constant from the EES back to the blood plasma while v_p is the plasma volume. Furthermore, $\circledast$ denotes the convolution operator.

From the other hand, PM ignores the transfer of CA from the EES back to blood plasma as compared to ETM and its equation is given by (7).

$$C_t(t) = K^{trans}\int_0^t C_a(\tau)d\tau + v_p C_a(t) \quad (7)$$

III. Results

Voxel based parametric maps of WIN and f-IVIM were produced at a parasagittal plane, normalization at the range of [0,1] served illustration purposes. Osseous areas appear black as expected as they show no enhancement in DCE sequences (Fig.3 [left]) and they exhibit mono-exponential DWI signal decay (Fig3. [right]). At the other end macroscopically perfusion areas (vessels) appear with high WIN and f values.

Regarding the fitting performance, $mean(\bar{R}^2) \pm std(\bar{R}^2)$ of the models for both DCE and DWI data over the whole patient cohort are presented in I. A Pearson's r of 0.582 was measured between f-IVIM method 1 and EMG while a slightly higher correlation was found for f-IVIM method 2 and EMG (r = 0.588) as shown in the third column of I. Indicative examples showing visual similarity between WIN-f method 1 and WIN-f method 2 are shown in Fig. 3 and Fig. 4. In addition, quantile-quantile plots (or scatter plots) are also appended in Fig.3 and Fig.4 to visually show the linear relationship between WIN and f-IVIM. It is important to note that the corresponding p-values per patient were significantly lower than 10^{-5} for all cases because the analysis was voxel based rather than averaged voxel values from a certain region of interest (ROI) based.

TABLE I. MODEL FITTING PERFORMANCE AND PEARSONS CORRELATION COEFFICIENT

Models/Methods	(mean) $\bar{R}^2 \pm$ (std($\bar{R}^2$))	Pearson's (r)
IVIM method 1	0.603 ± (0.306)	0.582
EMG	0.443 ± (0.332)	
IVIM method 2	0.587 ± (0.312)	0.588

IV. Discussion

The main goal of the present study was to investigate the correlation of perfusion related markers derived by different imaging techniques (DCE, DWI) which in turn can open new horizons in MRI perfusion imaging. In our case, patients with CLI are at a higher risk for amputation and require urgent revascularization by means of surgical or endovascular procedures [25]. For this reason, careful monitoring is necessary including baseline and frequent follow up examinations. In such cases, DWI perfusion may be an attractive alternative to DCE-MRI since it doesn't require contrast medium administration.

This work comes as an extension of a previously published paper reporting Pearson's r = 0.601 between f-IVIM method2 and relative enhancement ratio (RER) and r = 0.592 between f-IVIM method 2 and RER [13]. The WIN approach has significant advantages over the RER study because of the fitting procedure that eliminates noise contamination in the calculation of RER. However, the fact that both DCE derived semi-quantitative markers (WIN, RER) have positive correlation with DWI derived f-IVIM is

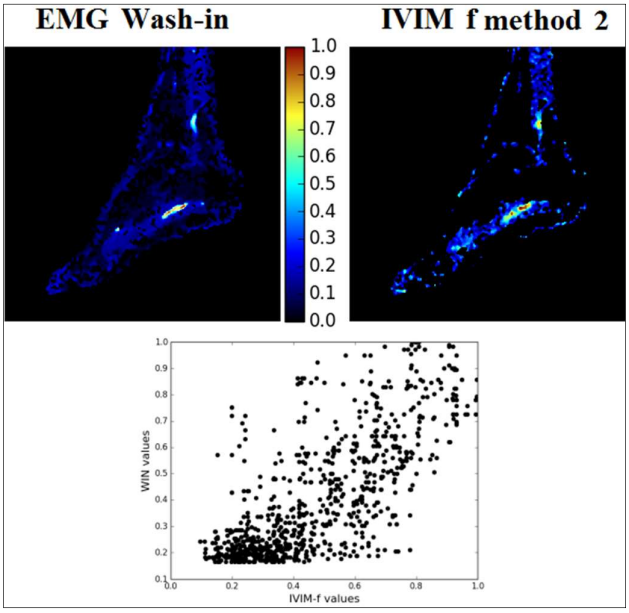

Fig. 4. DCE and DWI perfusion analysis of a patient with PAD. Parasagittal parametric map of the lower extremity showing Wash-In (WIN) calculated by EMG [upper left] and f-IVIM method 2 [upper right]. Both maps have been normalized to [0,1]. [Lower image:] q-q plot of WIN versus f-IVIM values.

an encouraging result further supporting the possible use of DWI MRI for perfusion imaging.

Both aforementioned works have a similar Pearson's r of the order of 0.6 which is considered as a positive correlation. This value of r is satisfactory considering that DWI and DCE are based on different physical properties and also differ significantly in the assumptions used for post processing. A perfect correlation cannot be expected, rather our aim is to prove that to a large extent the corresponding parametric images will convey similar information to the clinician. To support this statement, there is a large number of publications in clinical research reporting an r in the range of 0.5 to 0.7 which is considered as a good correlation although not strong [6]–[8]. It has to be noted that in this study we extended our dataset with 7 new cases.

Concerning the goodness of fit, a conclusion drawn from [13] was that compared to the widely used quantitative pharmacokinetic models, such as, ETM in (6) and PM in (7), semi-quantitative model EMG exhibits higher $\bar{R}^2$. This in turn can be attributed to reported variability of the Ktrans parameter across imaging centers using different computational steps and necessitating user interaction (subjective AIF), T1 mapping or constant T1, temporal resolution etc.). The final outcome is reported to vary as much as an order of magnitude across centers [22], [26]. On the contrary, EMG quantification is a one-step fitting process of EMG function to the temporal data. Moreover, the latter requires a simpler acquisition protocol without the need for dynamic sequences with variable flip angles (T1 mapping). To this end, we used semi quantitative pharmacokinetic models for quantification.

DWI acquisition is based on HASTE sequence avoiding thus fat suppression inherent in echo planar imaging (EPI) sequences usually used for diffusion [27], in order to avoid distortion artifacts and increase signal to noise ratio. Areas with no perfusion (cystic or osseous) are expected to have zero f (mono-exponential behavior) and appear black in Fig. 3[right] and Fig. 4 [right]. The same applies for areas with no enhancement in dynamic DCE images where flat time intensity curves result in zero WIN values.

A relatively slow injection rate of CA was chosen for two reasons during the dynamic phase. Firstly, muscles are normally characterized by slow perfusion rate which can be easily quantified using a slow injection rate. Secondly, a fast injection rate (bolus injection technique) induces susceptibility artifacts from the presence of highly concentrated contrast agent which in turn can be mitigated with the slow rate non-bolus administration.

Comparing DWI and DCE quantification methods, we observed higher $\bar{R}^2$ for the former. It has to be noted though that better $\bar{R}^2$ for DWI methods is also favored by the smaller number parameters for optimization (explanatory variables p in (4)) and therefore it affects the direct comparison of fitting performance. Moreover, another limitation of our study is the necessity of resizing the parametric maps through bicubic interpolation since matrix sizes for DCE and DWI raw data were different. Although the present study had a larger patient cohort compared to the previous one, it is still limited for a robust validation of our findings. It is within our future plans to expand this study to a larger patient cohort in order to increase the statistical power of our analysis and to perform in addition longitudinal studies following revascularization through endovascular stents [28].

ACKNOWLEDGMENT

The authors wish to acknowledge Professor *Thomas G. Maris* for MRI protocol optimization, Professor *Kostas Marias* for his support and guidance and MD *Galanakis Nikolaos* for his comments on clinical aspects.

REFERENCES

[1] M. Essig *et al.*, "Perfusion MRI: the five most frequently asked technical questions.," *AJR. Am. J. Roentgenol.*, vol. 200, no. 1, pp. 24–34, Jan. 2013.

[2] T. Nielsen, T. Wittenborn, and M. R. Horsman, "Dynamic Contrast-Enhanced Magnetic Resonance Imaging (DCE-MRI) in Preclinical Studies of Antivascular Treatments.," *Pharmaceutics*, vol. 4, no. 4, pp. 563–89, Nov. 2012.

[3] D. L. Le Bihan, Denis, Eric Breton, "Seperation of Diffusion and Perfusion in Intravoxel Incoherent Motion MR Imaging," *Radiology*, vol. 168, pp. 497–505, 1988.

[4] D.-M. Koh *et al.*, "Intravoxel Incoherent Motion in Body Diffusion-Weighted MRI: Reality and Challenges," *AJR*, vol. 196, pp. 1351–1361, 2011.

[5] H. S. Kim, C. H. Suh, N. Kim, C.-G. Choi, and S. J. Kim, "Histogram analysis of intravoxel incoherent motion for differentiating recurrent tumor from treatment effect in patients with glioblastoma: initial clinical experience.," *AJNR. Am. J. Neuroradiol.*, vol. 35, no. 3, pp. 490–7, Mar. 2014.

[6] C. Federau, K. O'Brien, R. Meuli, P. Hagmann, and P. Maeder, "Measuring brain perfusion with intravoxel incoherent motion (IVIM): Initial clinical experience," *J. Magn. Reson. Imaging*, vol. 39, no. 3, pp. 624–632, 2014.

[7] N. Fujima *et al.*, "Intravoxel incoherent motion diffusion-weighted imaging in head and neck squamous cell carcinoma: Assessment of perfusion-related parameters compared to dynamic contrast-enhanced MRI," *Magn. Reson. Imaging*, vol. 32, no. 10, pp. 1206–1213, Dec. 2014.

[8] S. Suo *et al.*, "Intravoxel incoherent motion diffusion-weighted MR imaging of breast cancer at 3.0 tesla: Comparison of different curve-fitting methods," *J. Magn. Reson. Imaging*, vol. 42, no. 2, pp. 362–370, 2015.

[9] G. S. Ioannidis, K. Nikiforaki, and A. Karantanas, "Statistical and spatial correlation between diffusion and perfusion MR imaging parameters: A study on soft tissue sarcomas," *Phys. Medica*, vol. 65, pp. 59–66, Sep. 2019.

[10] A. J. J. Wood and W. R. Hiatt, "Medical Treatment of Peripheral Arterial Disease and Claudication," *N. Engl. J. Med.*, vol. 344, no. 21, pp. 1608–1621, May 2001.

[11] G. Peach, M. Griffin, K. G. Jones, M. M. Thompson, and R. J. Hinchliffe, "Diagnosis and

management of peripheral arterial disease," *BMJ*, vol. 345, 2012.

[12] "Gadolinium-containing contrast agents | European Medicines Agency." [Online]. Available: https://www.ema.europa.eu/en/medicines/human/referrals/gadolinium-containing-contrast-agents. [Accessed: 19-Jun-2019].

[13] G. S. Ioannidis *et al.*, "A correlative study between diffusion and perfusion MR imaging parameters on peripheral arterial disease data," *Magn. Reson. Imaging*, vol. 55, pp. 26–35, Jan. 2019.

[14] R. FONTAINE, M. KIM, and R. KIENY, "[Surgical treatment of peripheral circulation disorders].," *Helv. Chir. Acta*, vol. 21, no. 5–6, pp. 499–533, Dec. 1954.

[15] H. Chang and J. M. Fitzpatrick, "A technique for accurate magnetic resonance imaging in the presence of field inhomogeneities," *IEEE Trans. Med. Imaging*, vol. 11, no. 3, pp. 319–329, 1992.

[16] M. A. Branch, T. F. Coleman, and Y. Li, "A Subspace, Interior, and Conjugate Gradient Method for Large-Scale Bound-Constrained Minimization Problems," *SIAM J. Sci. Comput.*, vol. 21, no. 1, pp. 1–23, Jan. 1999.

[17] T. O. Pearu Peterson, Eric Jones, "SciPy: Open source scientific tools for Python," 2001. [Online]. Available: http://www.scipy.org/.

[18] T. C. Kwee *et al.*, "Comparison of apparent diffusion coefficients and distributed diffusion coefficients in high-grade gliomas.," *J. Magn. Reson. Imaging*, vol. 31, no. 3, pp. 531–7, Mar. 2010.

[19] Y.-C. Hu *et al.*, "Intravoxel incoherent motion diffusion-weighted MR imaging of gliomas: efficacy in preoperative grading," *Sci. Rep.*, vol. 4, no. 16, p. 7208, 2014.

[20] D. W. Marquardt, "An Algorithm for Least-Squares Estimation of Nonlinear Parameters," *J. Soc. Ind. Appl. Math.*, vol. 11, no. 2, pp. 431–441, 1963.

[21] V. Savvopoulou, T. G. Maris, L. Vlahos, and L. A. Moulopoulos, "Differences in perfusion parameters between upper and lower lumbar vertebral segments with dynamic contrast-enhanced MRI (DCE MRI)," *Eur. Radiol.*, vol. 18, no. 9, pp. 1876–1883, Sep. 2008.

[22] G. S. Ioannidis, T. G. Maris, K. Nikiforaki, A. Karantanas, and K. Marias, "Investigating the correlation of Ktrans with semi-quantitative MRI parameters towards more robust and reproducible perfusion imaging biomarkers in three cancer types," *IEEE J. Biomed. Heal. Informatics*, pp. 1–1, 2018.

[23] P. S. Tofts *et al.*, "Estimating kinetic parameters from dynamic contrast-enhanced T(1)-weighted MRI of a diffusable tracer: standardized quantities and symbols.," *J. Magn. Reson. Imaging*, vol. 10, no. 3, pp. 223–32, Sep. 1999.

[24] C. S. Patlak, R. G. Blasberg, and J. D. Fenstermacher, "Graphical Evaluation of Blood-to-Brain Transfer Constants from Multiple-Time Uptake Data," *J. Cereb. Blood Flow Metab.*, vol. 3, no. 1, pp. 1–7, Mar. 1983.

[25] L. Norgren *et al.*, "Inter-Society Consensus for the Management of Peripheral Arterial Disease (TASC II)," *J. Vasc. Surg.*, vol. 45, no. 1, pp. S5–S67, Jan. 2007.

[26] C. S. Ng *et al.*, "Dependence of DCE-MRI biomarker values on analysis algorithm.," *PLoS One*, vol. 10, no. 7, p. e0130168, 2015.

[27] M. Poustchi-Amin, S. A. Mirowitz, J. J. Brown, R. C. McKinstry, and T. Li, "Principles and Applications of Echo-planar Imaging: A Review for the General Radiologist," *RadioGraphics*, vol. 21, no. 3, pp. 767–779, May 2001.

[28] N. Galanakis, N. Kontopodis, I. Peteinarakis, E. Kehagias, C. V. Ioannou, and D. Tsetis, "Direct Stenting in Patients with Acute Lower Limb Arterial Occlusions: Immediate and Long-Term Results," *Cardiovasc. Intervent. Radiol.*, vol. 40, no. 2, pp. 192–201, Feb. 2017.